Solid Freeform Fabrication 2017: Proceedings of the 28th Annual International Solid Freeform Fabrication Symposium – An Additive Manufacturing Conference
Reviewed Paper

Towards a Robust Production of FFF End-User Parts with Improved Tensile Properties

G. A. Mazzei Capote[1], A. Redmann[1], C. Koch[2] and N. Rudolph[1]

[1]Polymer Engineering Center, University of Wisconsin-Madison, Madison, WI 53706, USA
[2]RWTH Aachen University, 52062 Aachen, Germany

Abstract

The relatively low cost of Fused Filament Fabrication (FFF) printers and wide variety of materials -spanning multiple functionalities and prices- make this process interesting for production of functional parts. However, FFF produced objects underperform in terms of mechanical properties when compared to injection molding. Therefore, a study of tensile properties of FFF produced parts was conducted according to the ASTM D-638 standard, using a commercial and an in-house produced ABS filament. Initial tests using commercial ABS revealed poor reproducibility of results, which were analyzed in detail in this study. This led to designing a formal bed levelling procedure for the printer, evaluating effects of printer configuration and material quality as well as exploring modifications to the ASTM test procedure. As a result, test specimens with properties close to injection molding parts were produced. Therefore, the different impact factors will be discussed and the new procedures will be presented.

Keywords: 3D printing, FFF, Tensile properties

Introduction

Additive Manufacturing (AM) technologies excel at producing complex geometries that are normally infeasible through more conventional manufacturing techniques. Fused Filament Fabrication (FFF) in particular has been at the forefront of the AM technologies due to the advent of low-cost, desktop 3D printers in the early 2010s [1, 2, 3, 4]. The decreasing costs of desktop FFF printers, coupled with the constantly expanding availability of suitable materials, have slowly shifted the perception of FFF as a prototyping technique into a viable manufacturing technology [1].

While the prospect of using FFF to produce end user parts is attractive, this technology still faces the challenges and limitations that currently affect the field of AM as a whole. First and foremost, FFF parts -like all AM produced parts- tend to be highly anisotropic due to the layer by layer build approach [1, 2, 3, 5, 6, 7]. Secondly, standardized tests for AM technologies are still in the development stage [8, 9, 10]. This implies that predicting or verifying the mechanical performance of FFF produced parts can be difficult. Despite this, recent studies have shown that by manipulating raster orientation, part density and layer height, one can increase the tensile properties of FFF parts [1, 2, 8]. Most of these studies either used the ASTM D-638 Standard [11] directly, or based their custom testing procedures around it due to a lack of a better alternative. Since the geometry of the test coupons in this standard was designed to be produced via injection molding, a common adversity faced by researchers is the premature failure of samples in the

filleted section of the coupon due to stress concentrations inherent to the AM process. This is most prevalent in samples using a raster orientation parallel to the load direction [3, 4, 1, 10, 12].

Another problem that is inherent to FFF is the lack of information provided by commercial filament suppliers regarding material properties and extrusion processing conditions. Unlike in the more stablished plastics processing industry, where pellets are supplied with a datasheet that includes a plethora of material properties and recommended processing conditions, filament information is generally limited to recommended ranges for the printing and build plate temperatures. Since no datasheet is supplied with each spool of filament, there is no guarantee that two spools of material from the same manufacturer are identical. Additional tests are then required to assess material properties; usually involving grinding of the material beforehand.

Due to the challenges discussed above, this work aims to assess the possibility of producing reproducible tensile data from FFF produced coupons using the ASTM D-638 Type I specimen and exploring variations in the test geometry and gripping during testing. Two materials were used throughout the experiments: the first is a commercially available ABS and the second is filament extruded in-house using the SABIC Cyclolac™ MG94 resin.

Methodology:

1- Preliminary tests:

Coupons were printed following the ASTM D-638 Type I geometry using a Lulzbot® TAZ 5 printer using both single and dual nozzle print heads configured with a 0.5 mm nozzle. The necessary toolpath was generated using the SciSlice slicing engine developed at the University of Wisconsin-Madison [13]. Preliminary experiments were conducted with a commercially available, natural ABS manufactured by MatterHackers Inc. measuring 2.93 mm in diameter with an accuracy of ±0.07 mm as indicated by the manufacturer. In these experiments, the goal was to assess repeatability of results between different batches of samples produced with the same print parameters.

Four print conditions were selected based on the study of improvement of tensile properties of FFF parts performed by Koch in 2016 [1]. These four conditions involved the following printer parameters explained in detail below: layer height, bead orientation, and Extrusion Factor (EF).

Bead Orientation: The beads of the tensile specimens were oriented at an angle that was either parallel, perpendicular, or at 45° with respect to the load direction as shown in Figure 1. To minimize premature failure of the 0° samples due to stress concentrators in the filleted region, 13 shells were used for this raster orientation, and the wider shoulders were filled in the center.

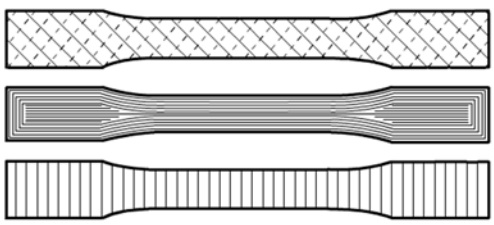

Figure 1: Schematic of raster orientation for printed Type I coupons. From top to bottom: ±45°,0° and 90°

Extrusion Factor (EF): EF represents a ratio of the area occupied by the cross section of a bead (A_{bead}) divided by the product of the bead width (W_{bead}) with the layer height (H_{layer}) as shown in Equation 1.

$$EF = \frac{A_{bead}}{W_{bead}.H_{layer}} \qquad \textit{Equation 1}$$

This factor is specified by the user in SciSlice and used to calculate the length of filament required to print a bead of known dimensions by using the volumetric balance shown in Equation 2. By varying the EF, one can significantly modify the structure of a bead, ranging from an ellipsoid (EF=π/4) to an almost filled rectangle (EF=1) as shown in Figure 2. With this in mind, the conditions chosen to assess batch reproducibility are shown in Table 1.

$$\frac{L_{filament}}{L_{bead}}.A_{filament} = EF.W_{bead}.H_{layer} \qquad \textit{Equation 2}$$

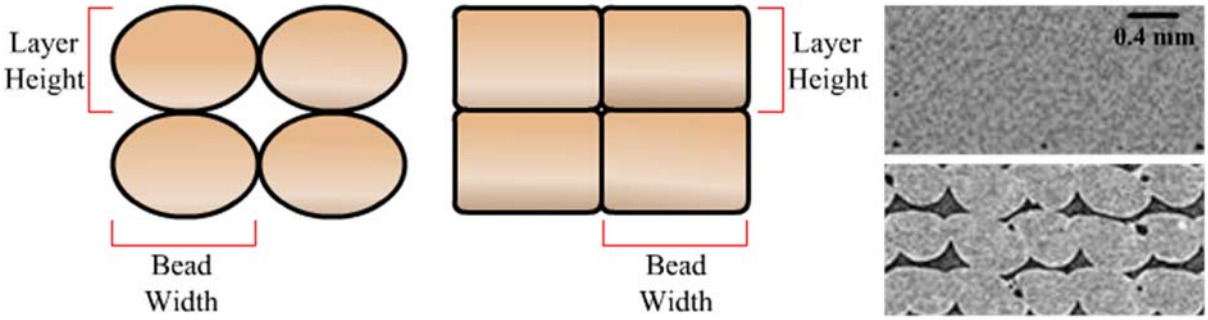

Figure 2: Comparison of beads produced with an EF of π/4 (left) and 1 (center). On the right are shown micro CT images of beads produced using an EF of 1 (top) and 0.8 (bottom)

Table 1: Batch reproducibility conditions for FFF tensile tests

Condition	Bead orientation	Layer height (LH) [mm]	Extrusion factor (EF)
1	0º	0.1	0.97
2	0º	0.3	1.01
3	45º	0.4	0.93
4	90º	0.3	1.02

Note that an extrusion factor greater than 1 simply implies that the part is slightly over extruded. The factors that were kept constant for all prints that use the Matterhackers filament are shown in Table 2:

Table 2: Constant print parameters throughout the reproducibility tests

Parameter	**Value**
Print Temperature	250 °C
Bed Temperature	110 °C
Print Speed	2000 mm/min

2- Extrusion of filament:

Since the use of a commercial filament does not guarantee constant properties throughout different spools, it is of interest to use a material of known processing conditions, dimensions and properties for this and future studies. Hence, making use of the extrusion capabilities present in the Polymer Engineering Center in the University of Wisconsin-Madison, a customized filament was extruded to be used in the research of mechanical properties of FFF parts.

The resin chosen to extrude filament was SABIC Cyclolac™ MG94. This is an ABS resin traditionally used for injection molding thin walled parts as well as FFF filament. With a reported Melt Flow Index of 11.7 g/10 min, it is an ideal resin for both the FFF and extrusion processes. Table 3 shows some of the material properties as reported by the manufacturer [14]:

Table 3: ABS Cyclolac™ MG94 properties

Property	Standard used	Reported value
Yield Stress	ASTM D-638	45.11 [MPa]
Failure Stress	ASTM D-638	34.32 [MPa]
Young's modulus	ASTM D-638	2471.28 [MPa]
Melt Flow Index	ASTM D-1238	11.7 [g/10 min]
Specific gravity	ASTM D-792	1.05 [-]

The extrusion setup consisted of a single screw extruder (Extrudex EDN 45X30D, Germany) with 45 mm screw diameter and L/D ratio of 30D. The hot melt is extruded at 205 ºC through a circular die with a 5.8 mm diameter. It is then guided through a pre-skinner into a vacuum-assisted, heated water bath (Conair, USA) to cool the extrudate whilst minimizing void formation. The solidified filament then passes through a 3-axis laser micrometer (LaserLinc, USA) and a belt puller (Conair, USA). The dimensions of the filament are adjusted in a control loop that allows adjustment of the pull speed to keep the extrudate within specification. The desired filament dimensions were a diameter of 2.85 mm with a tolerance of ±0.02 mm. In a last step, the filament is wound onto big spools. A schematic of the extrusion setup is shown in Figure 3.

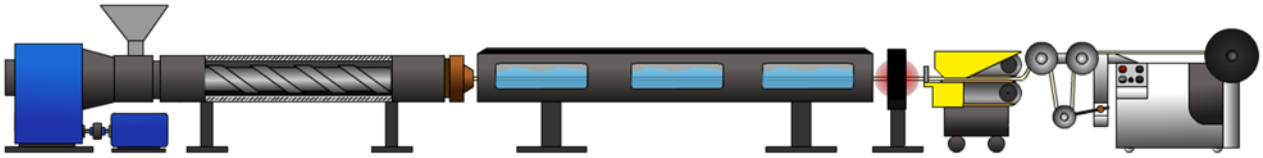

Figure 3: Extrusion setup schematic. From left to right: Extruder, Vacuum-assisted water bath, laser micrometer, puller, and filament winder.

An optimal printing temperature was then selected for this material. This was done following the pseudo-MFI test performed by Koch [1] and Pfeifer et al. [8] . In this test, the printer is instructed to extrude for 30 seconds at a theoretical volumetric flow of 400 mm^3/min, repeating this procedure through a range of temperatures between 190°C and 250°C and plotting the extruded mass as a function of temperature; see Figure 9 as example.

Finally, two sets of samples were printed in a randomized order following the conditions used for the Matterhackers material to assess repeatability.

Results and Discussion:

Three initial batches (p1, p2 and p3) of 5 specimens each were printed for preliminary tests, showing poor reproducibility of results. The yield stress of the printed parts fluctuated significantly, particularly in the 45° and 90° samples. By comparison, the 0° samples showed more consistent results; however, a common issue was failure of the test specimens outside of the gage section. A noteworthy result is that the samples printed with a 0° raster orientation, 0.1 mm LH, and an EF of 0.97, reached yield stresses comparable to injection molded samples. The bulk material was ground, injection molded and the Type V ASTM D-638 specimens were tested. The average yield stress was found to be 41.01 MPa. This implies that samples printed using condition 1 (Table 1) attained between 90 and 96% of the yield stress of the bulk material. All results are summarized in Figure 4.

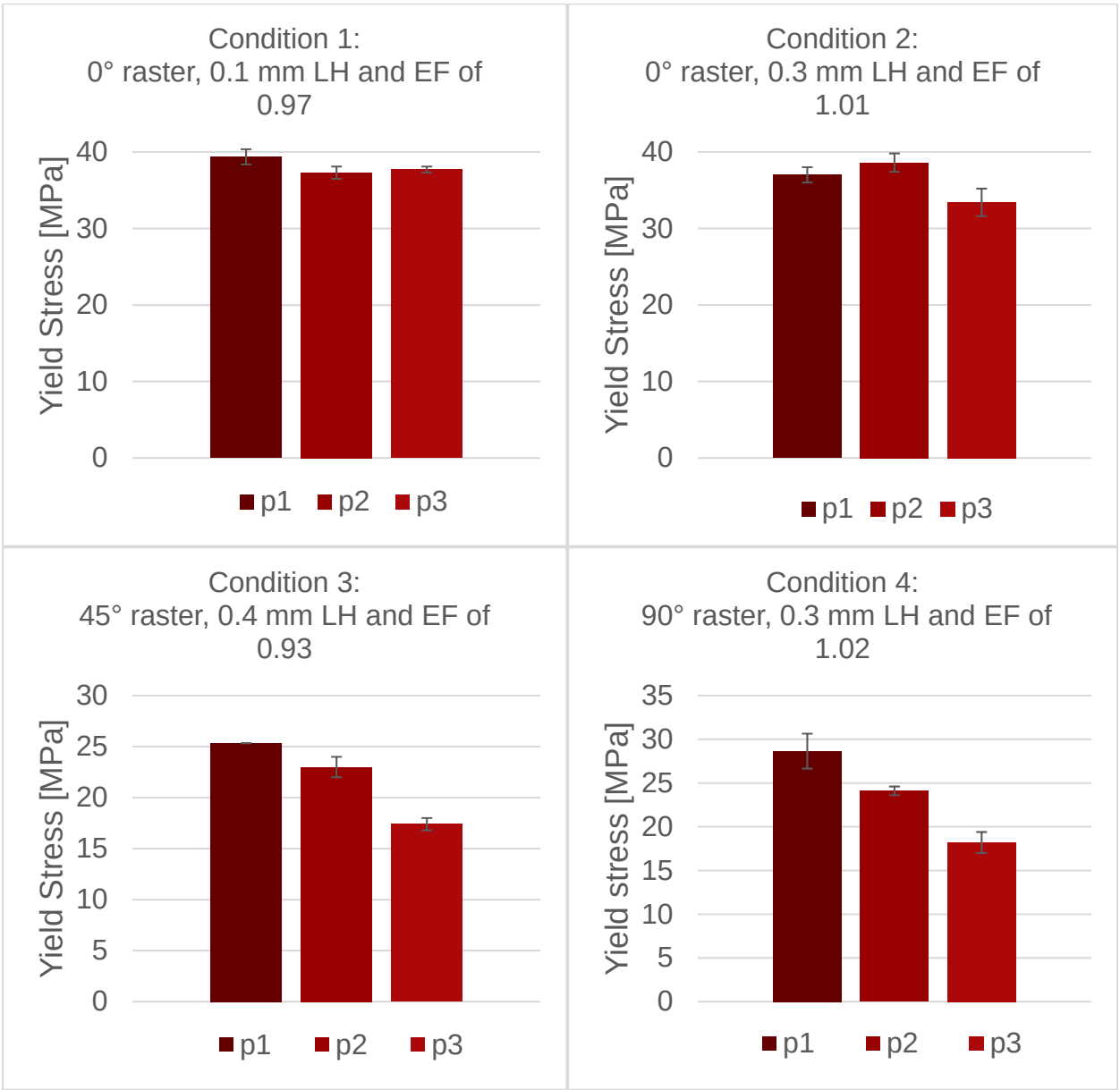

Figure 4: Batch consistency results with commercial filament. Batches p2 and p3 were printed using the dual nozzle print head.

The low reproducibility of results posed a challenge. Possible sources of error were identified as an uneven bed, the use of the dual nozzle print head and undesired additional stresses added during the testing procedure through the grips of the tensile test machine. According to Koch [1], an unlevelled bed can have a significant impact upon the mechanical properties of the final part since the first layers of the print won't have the desired solidity. To address this issue, a formal bed levelling procedure was designed using a flat top, push-in dial indicator with a resolution of 0.0005 in (0.0127 mm). The dial indicator was calibrated to show when the nozzle was a distance of 50 mm from the bed. Therefore, any deviation from this position would imply that the bed required adjustments on one of the four springs located at the corners of the build plate or the endstop located in the z axis of the machine. To ensure a level bed, an iteration of the levelling procedure requires 5 contact points with the indicator, as shown in Figure 5.

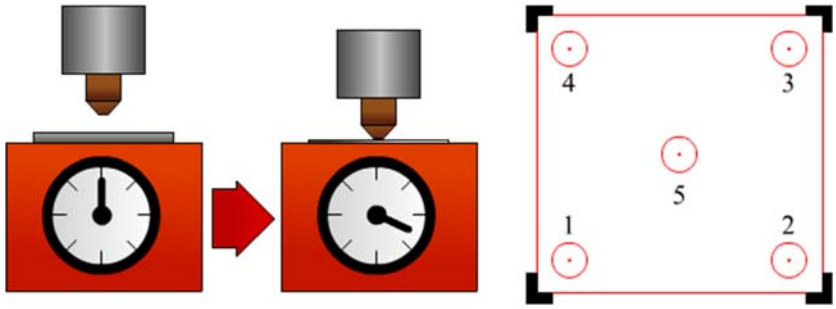

Figure 5: Bed levelling procedure using push in dial indicator. Points verified on the build plate shown on the right.

The dual nozzle print head vibrated throughout the prints due to its higher weight, larger dimensions and single anchor point and was thus substituted for a single nozzle print head. To minimize the additional stresses on the test coupons due to aggressive gripping, different tabbing configurations were tested. A similar approach has proven effective in the composites field as a mean to protect and properly transfer the load to test specimens [15]. The tabs considered were: wire mesh size 10 and size 14 as load transferring tabs, and emery cloth of grits 40,80 and 100 as protective tabs. Ten rectangular samples per tabbing condition were printed using a 0° orientation, LH of 0.3 mm, and EF of 1. As a control, 10 samples were also tested without tabbing. The desired outcome was to increase the percentage of samples breaking in the gage section. The test setup can be seen in Figure 6. A metal straight edge was used while clamping to minimize introduction of bending stresses upon the coupons during setup.

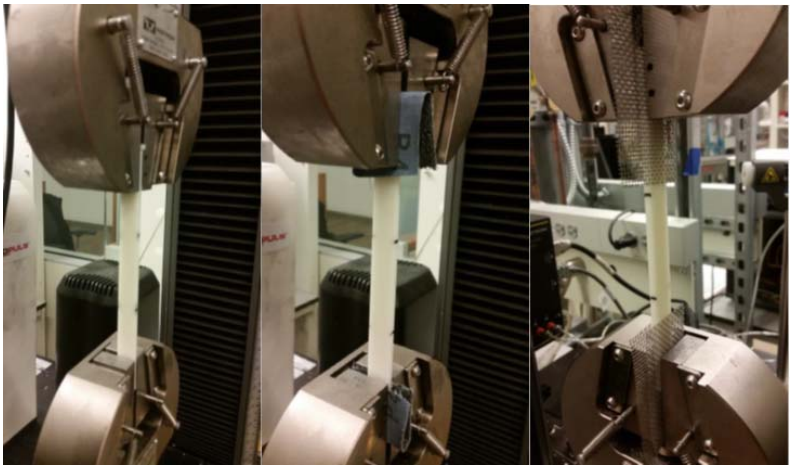

Figure 6: Specimen protection through tabbing. From left to right: No tabbing, emery cloth and wire mesh.

During testing, none of the control samples broke in the gage section, and the coupons with the wire mesh tabs consistently slipped out of the grips, thus rendering this option unusable. By comparison, the specimens protected with emery cloth showed an increase in the percentage of failure within the gage section. The results of these tests are summarized in Table 4.

Table 4: Tab protection results summary

Protection	Max stress [MPa]	Strain at break	Successful Tests [%]
None (control)	38.3±0.9	0.10±0.01	0
Emery Cloth 40 grit	37.4±1.1	0.13±0.04	20
Emery Cloth 80 grit	39.0±0.6	0.11±0.02	22
Emery Cloth 100 grit	38.5±1.1	0.12±0.03	56
10 wire mesh	NA	NA	NA
14 wire mesh	NA	NA	NA

These tests indicate that the use of a 100 grit emery cloth as specimen protection tabs increase the odds of failure in the gage section of the coupon and are therefore the recommended tabbing method. Following these findings, a 4th batch of 5 specimens (p4) was printed using the bed levelling procedure, a single nozzle print head, and tested using the 100 grit emery cloth as tab protection as shown in Figure 7. The results show a substantial increase in the yield stress of the 45° and 90° samples when compared to the tests that didn't use these considerations. The 0° samples failed more consistently within the gage section; however, no drastic change in the yield stress was observed. Figure 8 shows the results of these tests compared to p1, p2 and p3 which were tested without the bed levelling procedure nor tab protection.

Figure 7: Test setup with 100 grit emery cloth protection and extensometer.

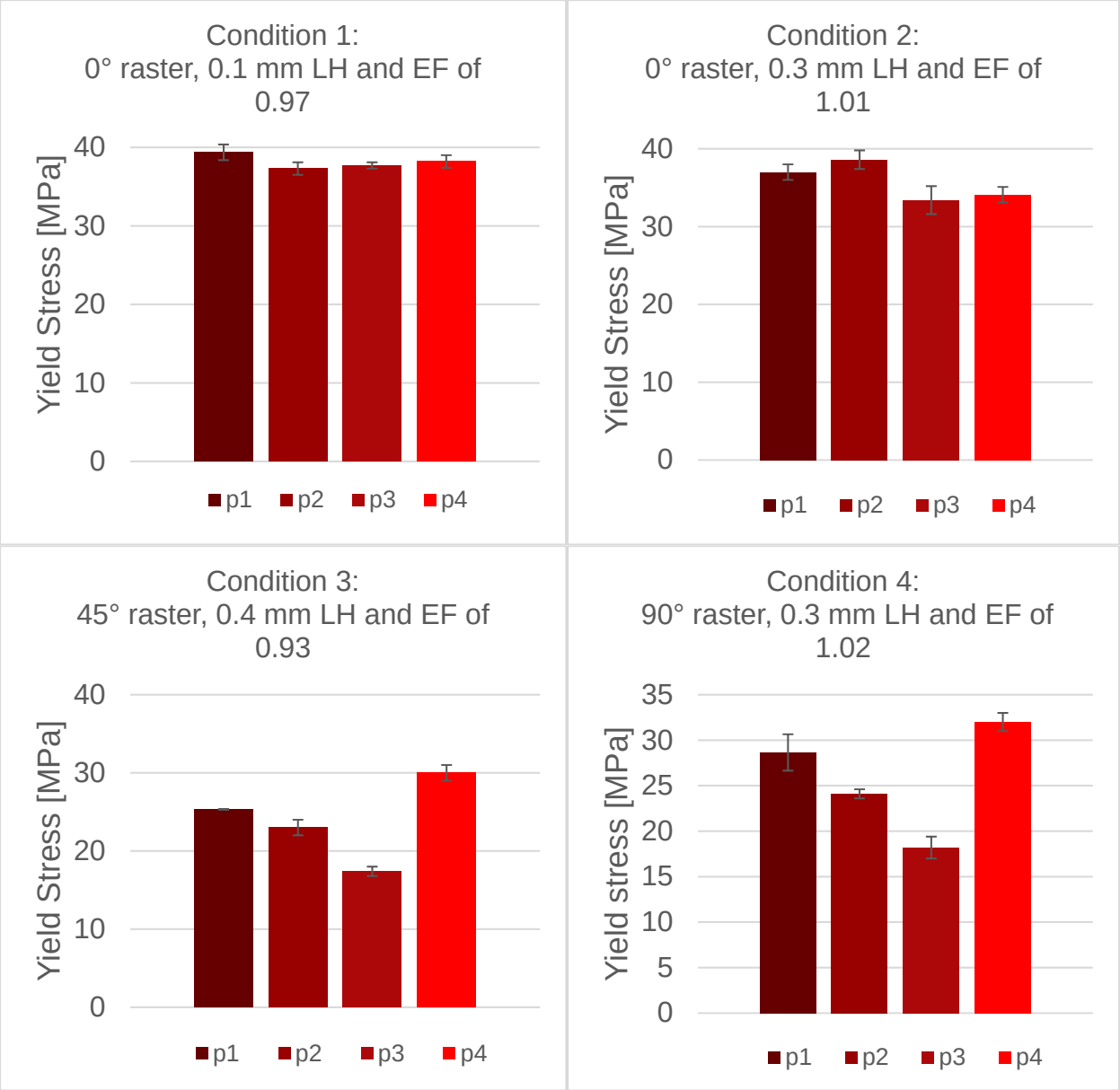

Figure 8: Yield stress results for all tested batches printed with commercial filament. p1 and p4 were printed using a single nozzle print head. p4 used bed levelling procedure and tab protection.

The effects of using a repeatable bed levelling procedure and tab protection through 100 grit emery cloth in conjunction with a single nozzle print head decrease premature failure of the samples. Following these findings with the Matterhackers filament, the logical next step was to apply this knowledge to samples printed with the extruded MG94 ABS material, since this eliminates concerns pertaining to material consistency throughout different spools of filament.

First and foremost, an appropriate print temperature needs to be selected. Following the execution of the pseudo-MFI test mentioned earlier, the graph depicted in Figure 9 was obtained. Using 1.04 g/cm^3 as the material density, the theoretical extruded mass corresponds to 208 mg.

The graph shows that this value is reached between 220 and 230°C. Using this finding, the print temperature for this material was selected as 230°C. Note that any print temperature below the 220-230°C threshold would imply producing under-extruded parts.

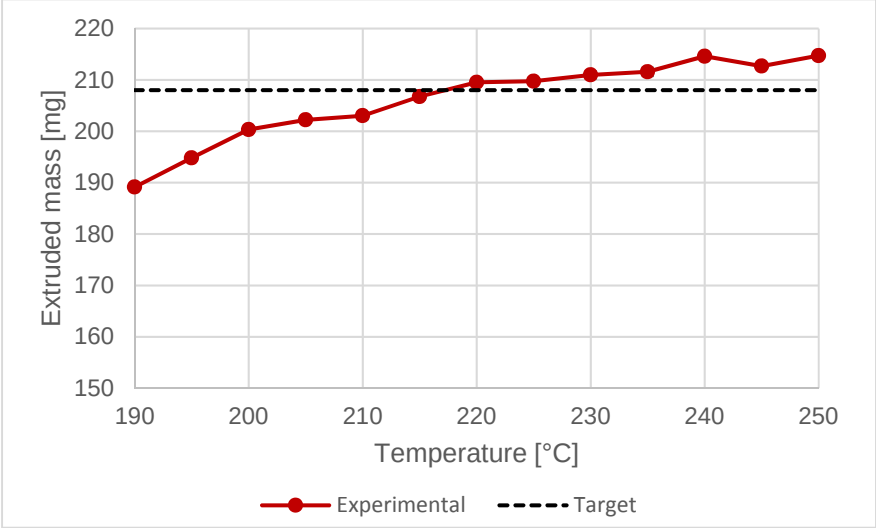

Figure 9: Extruded mass as a function of temperature for the extruded filament.

Following the selection of the print temperature, the print parameters shown in Table 5 were used to produce samples with the custom filament.

Table 5: Print parameters for custom filament

Parameter	Value
Print Temperature	230 °C
Bed Temperature	100 °C
Print Speed	2000 mm/min

To minimize unwanted effects stemming from lurking variables, a new nozzle was used to produce the samples and the print order was randomized as per Table 6. Both batches of 5 specimens each (o1 and o2) were produced using the single nozzle print head configuration.

Table 6: Print order for batches of coupons printed with custom filament

	Condition	o1 print order	o2 print order
1	0º, 0.1 mm LH, 0.97 EF	4	1
2	0º, 0.3 mm LH, 1.01 EF	1	3
3	45º, 0.4 mm LH, 0.93 EF	3	2
4	90º, 0.3 mm LH, 1.02 EF	2	4

The results of the tests can be seen in Figure 10. These show good agreement between o1 and o2 for all the conditions unlike in the preliminary tests. Once again, the 0° samples printed at a layer height of 0.1 mm and using an EF of 0.97 (condition 1) showed a yield stress that approaches that of the tested bulk material – using injection molded ASTM D-638 Type I

specimen- which has a yield stress of 42.4 MPa. In this case, the samples printed using these conditions attained between 94 and 97% of the yield stress of the bulk material.

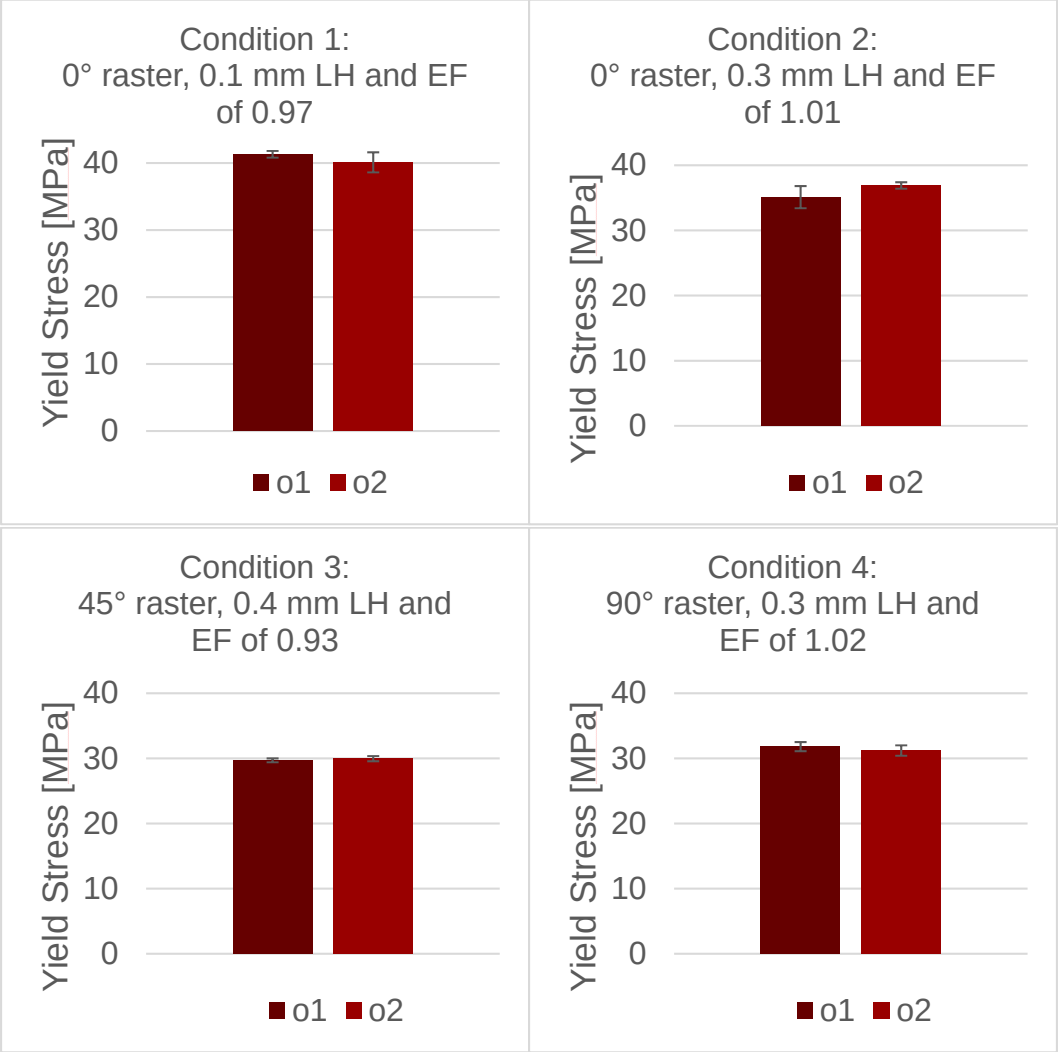

Figure 10: Batch consistency using custom filament

From these results, it becomes apparent that obtaining reproducible tensile data requires a combination of careful bed levelling and tab protection of the specimens to prevent premature failure of the coupons. It can also be seen that FFF parts can have performance that is competitive with injection molded parts if the bead orientation follows the direction of the load and a low layer height is used in conjunction with an extrusion factor that approaches 1. These findings can prove useful to a field where standardization of testing procedures is still being developed. Additionally, the use of custom extruded ABS eliminates the concerns pertaining to material consistency throughout different spools of commercial filament, thus making this the preferred material for future research.

Conclusions and Future Work:

This study managed to produce FFF parts with yield stresses that come within 90% or higher of its injection molded counterpart. However, attaining reproducible results required

designing a formal bed levelling procedure, protection of the test coupons through emery cloth tabs, and the use of a filament extruded in house -where processing conditions and dimensional tolerances are known and represent an advantage over most commercially available materials, where all this information is unknown to the user. Additional work needs to be done to further improve the failure rate inside the gage section of AM tensile specimen. Several potential solutions are being explored, including: glass fabric/epoxy laminate tabs, less aggressive gripping surfaces, and modified tensile specimen geometry.

These improvements open the possibility of confidently exploring other mechanical properties of printed parts -such as compressive and bending tests- and relationships between print parameters and final properties. A particular point of interest is studying the strength of the weld between the beads without the contribution of the turns -or edges- in 90° samples as a function of tool travel time and other factors that may influence the cooling of the molten plastic -such as print temperature and extrusion factor.

Acknowledgements

This material is based upon work supported by the National Science Foundation Graduate Research Fellowship Program under Grant No. DGE-1256259. Any opinions, findings, and conclusions or recommendations expressed in this material are those of the authors and do not necessarily reflect the views of the National Science Foundation. Additionally, support was also provided by the Graduate School and the Office of the Vice Chancellor for Research and Graduate Education at the University of Wisconsin-Madison with funding from the Wisconsin Alumni Research Foundation.

References

[1] C. Koch, "Fused Filament Fabrication (FFF) Optimization: Mechanical Anisotropy and Solidity Effects in Additive Manufacturing", M.S. thesis, Mech. Engr. Dept., Univ. of Wisconsin-Madison, Madison, WI, 2016.

[2] C. Koch, L. Van Hulle and N. Rudolph, "Investigation of mechanical anisotropy of the fused filament fabrication process via customized tool path generation," *Additive Manufacturing,* vol. 16, pp. 138-145, 2017.

[3] B. Rankouhi, S. Javadpour, F. Delfainan and T. Letcher, "Failure Analysis and Mechanical Characterization of 3D Printed ABS With Respect to Layer Thickness and Orientation," *Journal of Failure Analysis and Prevention,* vol. 16, no. 3, pp. 467-481, 2016.

[4] T. Letcher, B. Rankouhi and S. Javadpour, "Experimental study of mechanical properties of additively manufactured ABS plastic as function of layer parameters," in *ASME 2015 International Mechanical Engineering Congress and Exposition*, Houston, 2015.

[5] T. Mulholland, A. Falke and N. Rudolph, "Filled Thermoconductive Plastics for Fused Filament Fabrication," in *Annual International Solid Freeform Fabrication Symposium*, Austin, 2016.

[6] J. Bartolai, T. W. Simpson and R. Xie, "Predicting Strength of Thermoplastic Polymer Parts Produced Using Additive Manufacturing," in *Annual International Solid Freeform Fabrication Symposium*, Austin, 2016.

[7] S.-H. Ahn, M. Montero, D. Odell, S. Roundy and P. K. Wright, "Anisotropic material properties of Fused Deposition Modeling ABS," *Rapid Prototyping Journal,* vol. 8, no. 4, pp. 248-257, 2002.

[8] T. Pfeifer, C. Koch, L. Van Hulle, G. A. Mazzei Capote and N. Rudolph, "Optimization of the FDM™ Additive Manfucatring Process," in *SPE ANTEC*, Indianapolis, 2016.

[9] A. Lanzotti, D. M. Del Giudice, A. Lepore, G. Staiano and M. Martorelli, "On the Geometric Accuracy of RepRap Open-Source Three-Dimensional Printer," *Journal of Mechanical Design,* vol. 137, no. 10, pp. 101703-101703-8, 2015.

[10] A. R. Torrado and D. A. Robertson, "Failure Analysis and Anisotropy Evaluation of 3D-Printed Tensile Test Specimens of Different Geometries and Print Raster Patterns," *Journal of Failure Analysis and Prevention,* vol. 16, no. 1, pp. 154-164, 2016.

[11] ASTM International, *"Standard test method for tensile properties of plastics" ASTM D638-14,* West Conshohocken, PA, 2014.

[12] D. Croccolo, M. De Agostinis and G. Olmi, "Experimental characterization and analytical modelling of the mechanical behaviour of fused deposition processed parts made of ABS-M30," *Computational Material Science,* vol. 79, pp. 506-518, 2013.

[13] L. Van Hulle, "SciSlice: The Scientific Slicer," [Online]. Available: https://github.com/VanHulleOne/SciSlice. [Accessed 1 June 2017].

[14] N.N., Material information, *CYCOLAC™ Resin MG94,* Saudi Basic Industries Corporation (SABIC), 2016.

[15] D. O. Adams and D. F. Adams, "Tabbing guide for Composite Test Specimens," U.S. Department of Transportation- Federal Aviation Administration, Washington DC, 2002.